



Synthesis and mechanistic studies of novel spin-labeled combretastatin derivatives as potential antineoplastic agents



Ying-Qian Liu^{a,*}, Xiao-Jing Li^a, Chun-Yan Zhao^a, Xiang Nan^a, Jing Tian^a, Susan L. Morris-Natschke^b, Zhi-Jun Zhang^a, Xiao-Ming Yang^b, Liu Yang^d, Lin-Hai Li^a, Xing-Wen Zhou^a, Kuo-Hsiung Lee^{b,c,*}

^a School of Pharmacy, Lanzhou University, Lanzhou 730000, PR China

^b Natural Products Research Laboratories, UNC Eshelman School of Pharmacy, University of North Carolina, Chapel Hill, NC 27599-7568, United States

^c Chinese Medicine Research and Development Center, China Medical University and Hospital, Taichung, Taiwan

^d Environmental and Municipal Engineering School, Lanzhou Jiaotong University, Lanzhou 730000, PR China

ARTICLE INFO

Article history:

Received 10 October 2012

Revised 10 December 2012

Accepted 20 December 2012

Available online 9 January 2013

Keywords:

Combretastatin

Spin-labeled

Nitroxide

Cytotoxicity

Mechanistic analysis

ABSTRACT

Two series (**14a–d** and **21a–h**) of novel spin-labeled combretastatin derivatives were synthesized and evaluated for cytotoxicity against four tumor cell lines (K562, SGC-7901, Hela and HepG-2). Simultaneously, a representative compound **21a** was selected to investigate the antitumor mechanisms of these synthetic compounds. The results indicated that some of the compounds showed significant cytotoxicity against four tumor cell lines in vitro and were more active than etoposide, a clinically available anticancer drug. Among the newly synthesized compounds, **21a**, **21b** and **21c** displayed the greatest cytotoxicity against three tested tumor cell lines (HEPG-2, BGC-832 and Hela), with IC₅₀ values ranging from 0.15 to 1.05 μM, compared with values of 0.014–0.403 μM for 3-amino-deoxycombretastatin A-4 (**3**). In addition, the mechanistic analysis revealed that compound **21a** effectively interfered with tubulin dynamics to prevent mitosis in cancer cells, leading to cell cycle arrest and, eventually, dose dependent apoptosis.

© 2013 Elsevier Ltd. All rights reserved.

1. Introduction

Combretastatin A-4 (CA-4, **1**), isolated from the bark of the South African tree *Combretum caffrum*, is a highly effective natural tubulin-binding stilbenoid. It affects microtubule dynamics by binding to the colchicine site, and shows potent cytotoxicity against a wide variety of human cancer cell lines, including those that are multidrug resistant.^{1–3} The relative molecular simplicity of this compound coupled with its strong potency against cancer cell lines has stimulated significant interest in a numerous diverse ligands designed to mimic **1**. In recent years, such efforts have been devoted to detailed studies of the structure–activity relationships (SAR) of variously substituted stilbenes, as well as water-soluble prodrugs. Among the research highlights, the sodium phosphate prodrug (CA-4P, **2**) and other derivatives, including 3-amino-deoxycombretastatin A-4 (AVE8063, **3**), the amino acid derivative AC-7739 (**4**), the dihydroxy derivative CA-1 (**5**), and its sodium diphosphate prodrug CA-1P (**6**, OXI-4503) (Fig. 1), represent promising drugs in various clinical studies. These compounds can potently disrupt vasculature and significantly reduce a tumor's blood flow.^{4,5} From these investigations, we noticed that (a) the (Z)-configuration of the olefin bridge is essential for biological

activity and (b) a substituent at the 3'-position of the B-ring was almost always necessary for significant cytotoxic activity.⁶ These critical SAR findings prompted us to select 3'-amino-deoxycombretastatin A-4 (AVE8063, **3**) as a logical starting point in our continuing pursuit of novel anticancer chemotherapeutics.

Furthermore, the introduction of a stable nitroxyl radical into pharmaceutical molecules can cut down the toxicity and potentiate the antitumor effects to a certain degree. Some studies have shown that the introduction of nitroxyl moiety can lead to fast decomposition, higher alkylating and lower carbamoylating activity, better antimelanomic activity, lower general toxicity, and the ability to transport through cell membranes, while the nitroxyl free radicals themselves possess low toxicity and are not mutagenic or carcinogenic.^{7–11} In our prior studies, we prepared numerous spin-labeled compounds that displayed significant antineoplastic activity with markedly decreased toxicity compared with their parent compound.^{12–18} Among the tested compounds, GP-11 (**8**), a derivative of podophyllotoxin (**7**) (Fig. 1), was reported as a low immunosuppressive antitumor agent, which increased the mitotic index and resulted in G₂/M and, to a lesser extent, S arrest. GP-11 may possibly become a new antitumor agent with improved bioactivity and low toxicity. More recently, we also found the introduction of nitroxyl radical into the molecule of combretastatin A-4 potentiate its cytotoxic effect and some of these derivatives exhibited more potent activity than the clinical drug irinotecan.¹⁹ Inspired by this

* Corresponding authors. Tel.: +1 919 962 0066; fax: +1 919 966 3893.

E-mail addresses: yqliu@lzu.edu.cn (Y.-Q. Liu), khlee@unc.edu (K.-H. Lee).

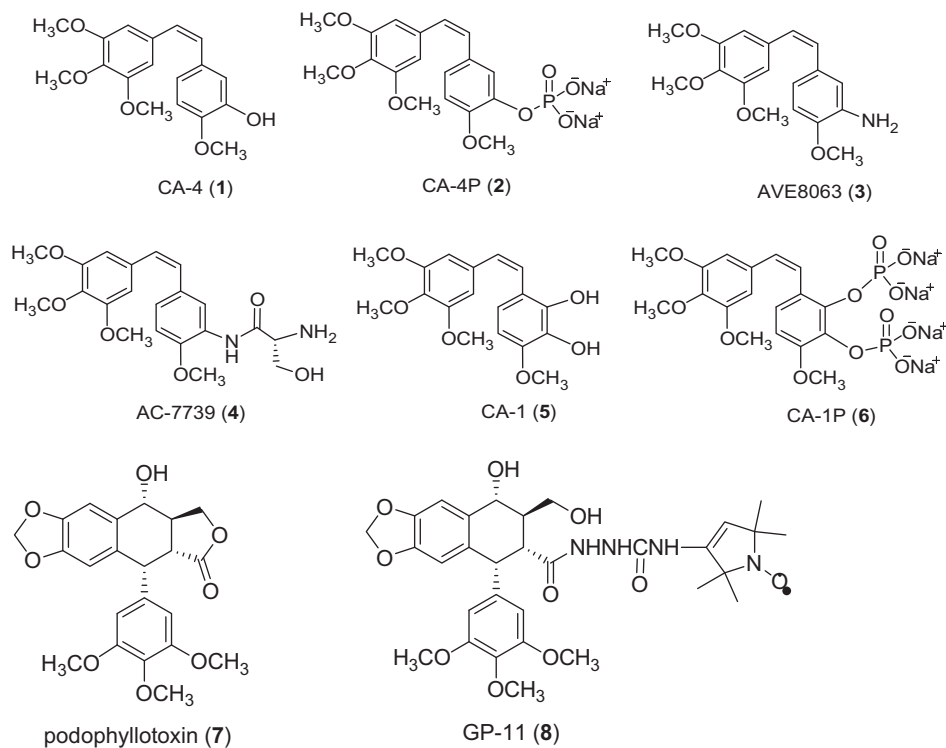


Figure 1. Structures of CA-4 (1), CA4P (2), AVE8063 (3), AC-7739 (4), CA-1 (5), CA-1P (6), podophyllotoxin (7) and GP-11(8).

prior work, we herein describe the synthesis and mechanistic studies of two novel series of derivatives of AVE8063 (3) as part of our continuing search for promising natural product-derived anticancer agents.

2. Results and discussion

2.1. Chemistry

As shown in Figure 2, compound **12** was obtained via the Perkin condensation^{20,21} of commercially available 3,4,5-trimethoxyphenylacetic acid (**9**) and 4-methoxy-3-nitrobenzaldehyde (**10**),

followed by decarboxylation of the corresponding acrylic acid **11** using copper and quinoline. In this reaction, only the pure *cis*-isomer was obtained in 52% yield after purification of the crude precipitate by fractional crystallization. The resulting compound **12** was reduced with zinc powder and acetic acid to afford the key intermediate **3**. Compound **3** was then condensed with the appropriate piperidine (pyrroline) nitroxyl acids (**13a–d**) in the presence of *N,N*-dicyclohexylcarbodiimide (DCC) and 4-dimethylaminopyridine (DMAP) to provide target compounds **14a–d**.

Based on previous work,^{16,17} as well as the facts that L-amino acids are actively transplanted into mammalian tissues, have good

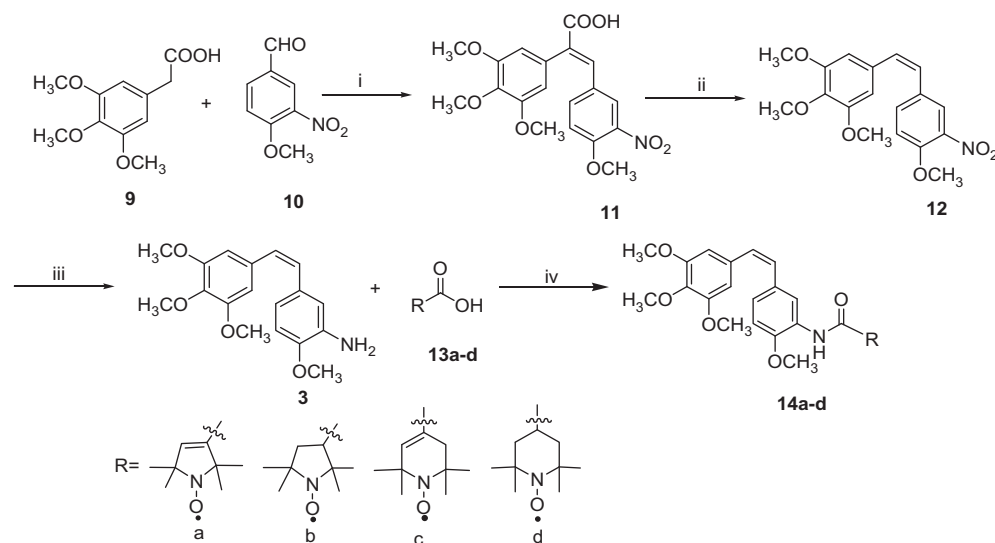


Figure 2. Synthesis of compounds **14 a–d**. Reagents and conditions: (i) $\text{Ac}_2\text{O}/\text{Et}_3\text{N}$, 140 °C; (ii) $\text{Cu}/\text{quinoline}$, 230 °C; (iii) Zn/HOAc , 24 h; (iv) $\text{DCC}/\text{DMAP}/\text{CH}_2\text{Cl}_2$.

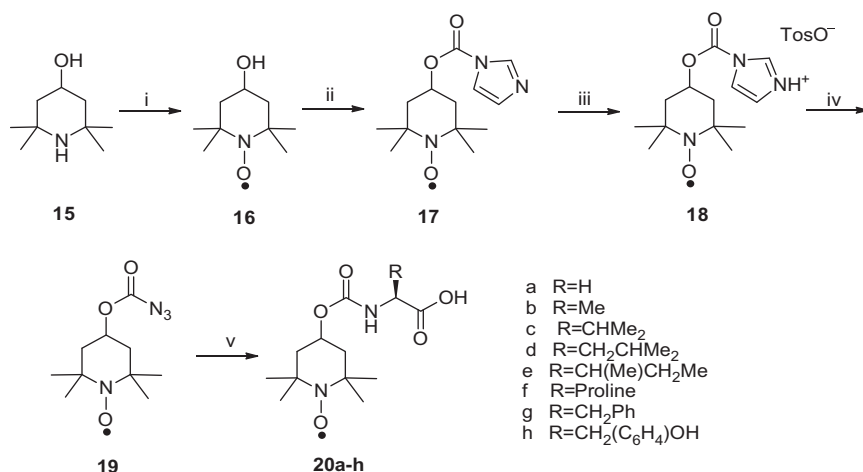


Figure 3. Synthesis of compounds **20a–h**. Reagents and conditions: (i) Na₂WO₄/H₂O₂/EDTA; (ii) *N,N*-carbonyl-diimidazole/THF; (iii) *p*-toluenesulfonic acid monohydrate; (iv) NaN₃/H₂O; (v) amino acids/MgO, 24 h.

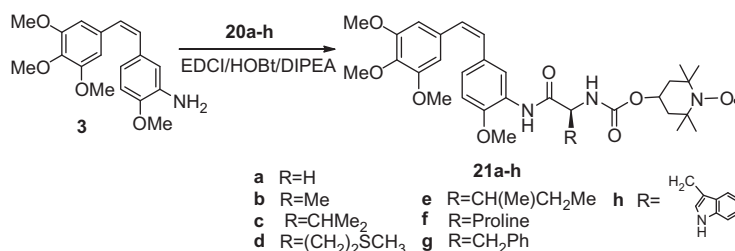


Figure 4. Synthesis of compounds **21a–h**.

water solubility, and are often used as carrier vehicles for some drugs, we also used an amino acid spacer as a linkage between the amino-combretastatin core (**3**) and the nitroxyl radical moiety. The starting materials, *N*-(1-oxyl-2,2,6,6-tetramethyl-4-piperidinyl-oxycarbonyl) amino acids **20a–h**, for the preparation of the target compounds **21a–h** were synthesized according to our previous procedure as shown in Figure 3.²² Briefly, 4-hydroxy-2,2,6,6-tetramethylpiperidine (**15**) was prepared by catalytic oxidation of 4-hydroxy-2,2,6,6-tetramethylpiperidine (**15**) with sodium tungstate–hydrogen peroxide–EDTA in 85% yield. Subsequently, the reaction of **16** with *N,N*-carbonyldiimidazole gave *N*-(1-oxyl-2,2,6,6-tetramethylpiperidinyl oxycarbonyl)-imidazole (**17**). Without further purification, compound **17** was reacted with *p*-tol-

uenesulfonic acid monohydrate to give its more reactive tosylate (**18**). Compound **18** was converted instantaneously into the corresponding alkoxy carbonyl azide (**19**) when dissolved in an aqueous solution of sodium azide. Compounds **20a–h** were obtained in good yields by reaction of **19** with various amino acids in the presence of MgO (Fig. 3). The desired compounds **21a–h** were produced by treating compound **3** with the corresponding [*N*-(1-oxyl-2,2,6,6-tetramethyl-4-piperidinyl-oxycarbonyl) amino acids **20a–h**] using *N*-ethyl-*N*-(3-dimethylaminopropyl)carbodiimide hydrochloride (EDCI) as the coupling agent (Fig. 4). All synthesized target compounds **14a–d** and **21a–h** were purified by column chromatography and their structures were confirmed from melting point, IR, ESR and HRMS analyses.

2.2. Biological assay

2.2.1. Cytotoxicity of compounds **14a–d** and **21a–h** against four cancer cell lines

Target compounds **14a–d** and **21a–h** were evaluated for in vitro cytotoxicity against the four tumor cell lines mentioned previously using an MTT assay with triplicate experiments.²³ Compound **3** and etoposide were used as positive controls. The screening results are shown in Table 1.

Although compounds **14a–d** and **21a–h** exhibited lower cytotoxicity than **3**, the common parent core, many of the synthesized compounds showed greater cytotoxicity than etoposide, a clinically available drug, against certain tumor cell lines in vitro. Compounds **21a**, **21b**, and **21c** exhibited the greatest cytotoxicity against three tested tumor cell lines (HEPG-2, BGC-832, and HeLa), with IC₅₀ values ranging from 0.15 to 1.05 μM.

From the screening results, conversion of **3** into the spin-labeled compounds **14a–d** increased the IC₅₀ values greatly. These results

Table 1
In vitro cytotoxicity against four tumor cell lines

Entry	IC ₅₀ (μM)			
	K-562	HEPG-2	BGC-832	HeLa
3	0.12	0.028	0.014	0.403
14a	>100	38.76	>100	42.26
14b	10.38	24.97	4.93	7.60
14c	15.62	10.70	6.21	8.57
14d	16.95	51.25	42.54	59.22
21a	1.09	0.98	0.39	0.41
21b	1.56	0.73	0.96	0.39
21c	11.98	1.05	0.43	0.15
21d	4.15	2.05	1.68	1.16
21e	18.77	2.19	3.07	2.33
21f	5.53	4.48	4.71	3.39
21g	5.80	0.28	6.33	8.37
21h	0.56	2.27	3.55	2.08
Etoposide	2.85	103.81	26.85	17.68

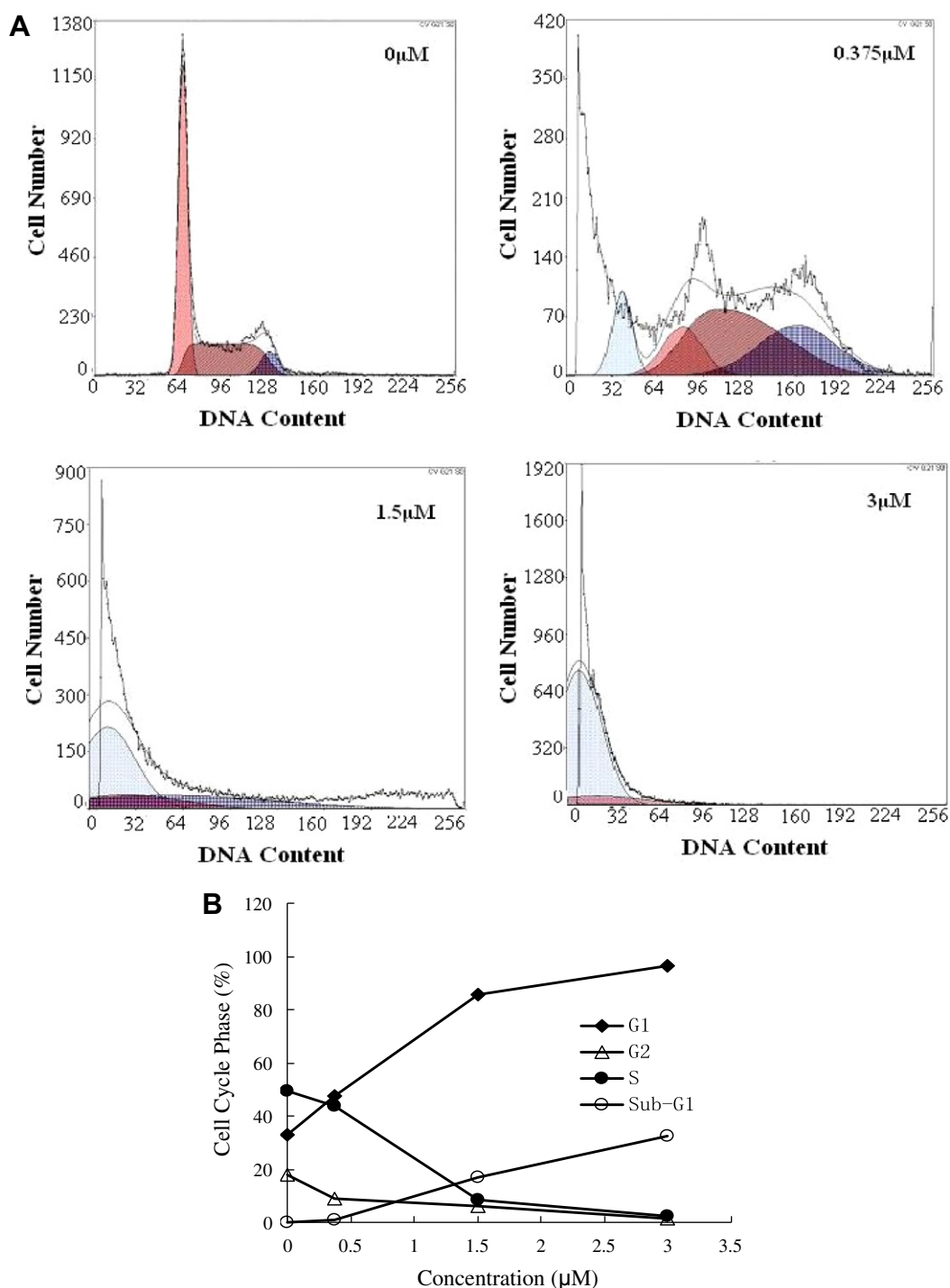


Figure 5. Effects of compound **21a** on the cell cycle distribution of HeLa cells. The cells were cultured for 36 h without the compound or with compound **21a** at 0.375, 1.5 and 3 μ M (A) inhibition of cell growth; (B) quantitative analysis of cell cycle phase.

indicated that the cytotoxic profile may be sensitive to the size and electronic density of the nitroxide substituents at the NH_2 group of **3**. However compounds **21a–h** with an amino acid linker between the nitroxide moiety and the core of **3** showed significantly improved cytotoxic activity against all four tested tumor cell lines compared to compounds **14a–d**. From an SAR consideration, the structures of the amino acid linkages between the core and nitroxide moieties affected the inhibitory activity against four tumor cell lines in vitro. Compounds **21a** (glycine spacer) and **21b** (alanine spacer) exhibited IC_{50} values between 0.39 and 1.56 μ M against all four cell lines. Compound **21c** (valine spacer) was significantly

active against all cell lines, except for K-562. Compounds **21d** (methionine spacer) and **21e** (isoleucine spacer) showed the same trend, but were slightly less potent than **21c**. Compounds **21f** (proline spacer), **21g** (phenylalanine spacer), and **21h** (tryptophan spacer) generally were less potent, with two exceptions. Compound **21h** showed the highest potency (IC_{50} 0.56 μ M) against K-562, and **21g** showed the highest potency (IC_{50} 0.28 μ M) against HEPG-2. These differences could be ascribed to a combination of factors, such as the nature of the substituents (e.g., size, electronic characteristics, and other factors) or by a different in interaction at the active site. This investigation highlighted that the identity of

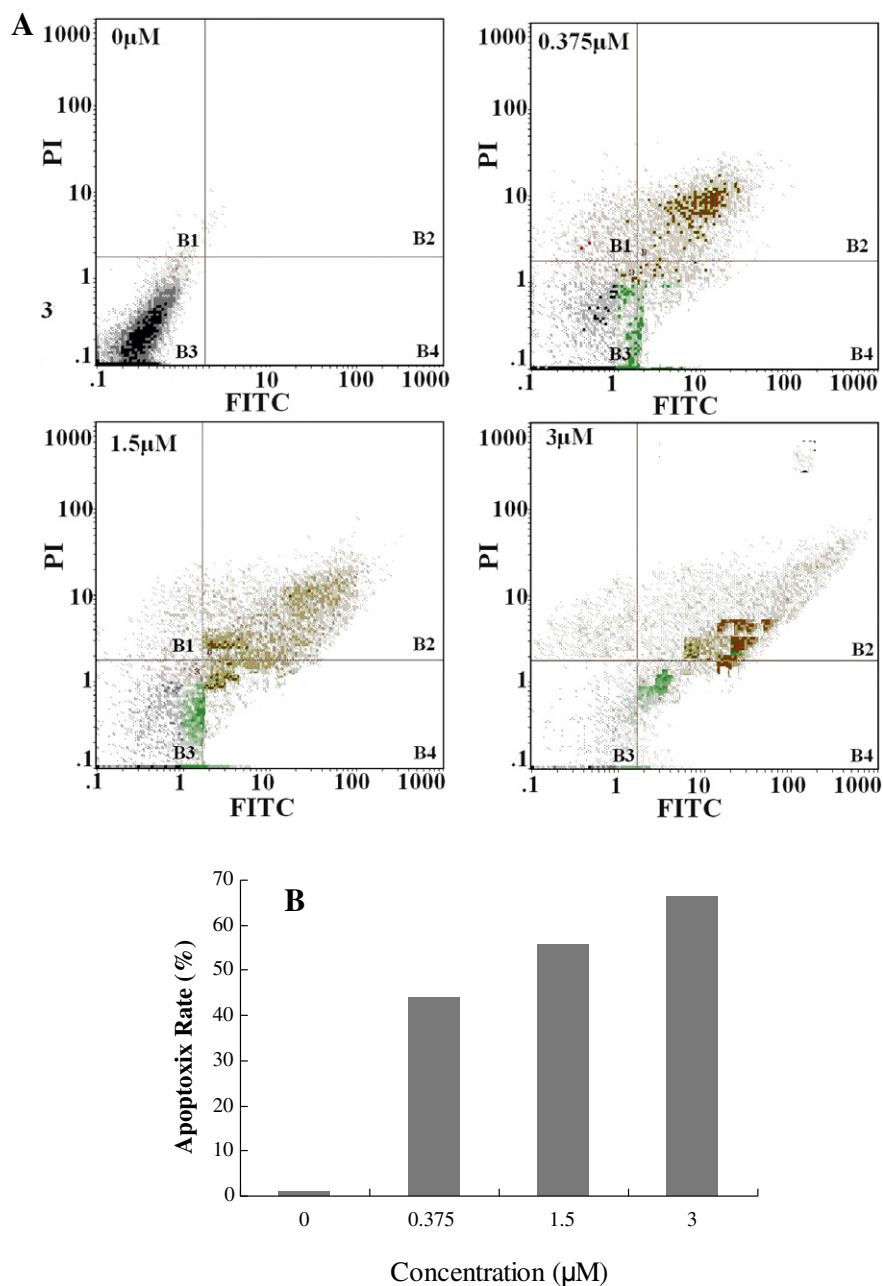


Figure 6. (A) Apoptotic effects on human leukemia HeLa cell line induced by compound **21a**. The cells were incubated in media containing various concentration of **21a** (0, 0.375, 1.5 and 3 μM) for 24 h. Cells and the amount of apoptotic cells were determined by flow cytometry using FITC-Annexin V/PI staining. (B) The rate of apoptotic cells as detected by flow cytometry. Cells in B1 and B2 quadrants were considered to be apoptotic cells. The experiment was repeated three times.

the amino acid spacers had a major impact on cytotoxic activity of such analogues. Hence, a systemic, predictable correlation could be made between the nature of the amino acids and antitumor activity.

2.2.2. Analysis of cell cycle

On the basis of the above results, it was found that compound **21a** significantly inhibited the growth of four human cancer cell lines. To determine whether the antitumor effects of these compounds were caused by cell cycle accumulation at a certain phase, the effects of **21a** on cell cycle progression were also determined by flow cytometry analysis in HeLa cells cultured for 36 h in the presence of increasing concentrations of compound **21a** (0, 0.375, 1.5, and 3 μM). As shown in Figure 5, treatment with 0.375, 1.5,

and 3 μM of **21a** led to accumulation of cells in the G1 phase; 32.85%, 85.82%, and 96.25%, respectively, of the cells were in G1 phase, compared with 47.36% in untreated cultures. In parallel to the G1 block, the cell cycle analysis showed a clearly increased proportion of sub-G1 cells, which is regarded as a characteristic of apoptotic cells. In untreated cultures, only 0.20% of the cells were in sub-G1 phase, whereas 1.14%, 16.71%, and 32.42% of cells were in the sub-G1 phase after 36 h treatment with 0.375, 1.5, and 3 μM of compound **21a**, respectively. These data demonstrated that **21a** can induce G1 arrest and apoptosis in HeLa cells. In addition, a simultaneous sharp decrease in S and G2 cells occurred. All effects were observed in a dose-dependent manner. These results demonstrated that **21a** interferes with cell proliferation by arresting the cell cycle in a certain phase.

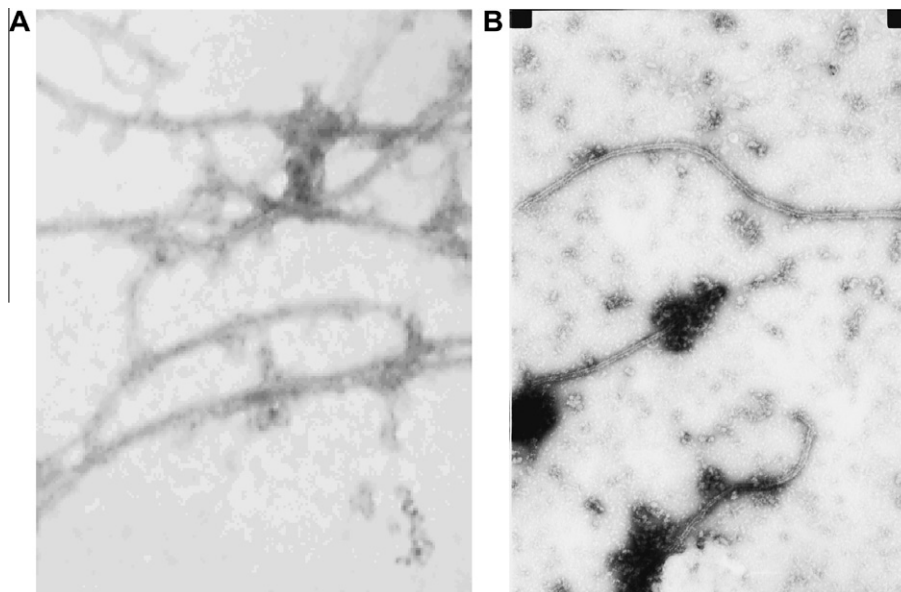


Figure 7. (A) Normal interphase microtubules; (B) loss of interphase microtubules induced by compound **21a**.

2.2.3. Effects on apoptosis

In addition, to determine whether compounds exhibiting high antitumor activity induce apoptosis of HeLa cells, the cells were treated with the active compound **21a** to measure the induction of cell death. After exposure to compound **21a** for 24 h, flow cytometry using the FITC-Annexin V/PI double staining method was used to generate an apoptotic cell scatterplot of the control group and the groups treated with compound **21a**. As shown in Figure 6, B1 quadrant presented the late apoptotic cells, B2 quadrant presented the early apoptotic cells, B3 quadrant presented the living cells, and B4 quadrant presented the damaged cells. With the increasing concentration of compound **21a**, the percentage of the early apoptotic cells increased from 0.17% to 52.6%, together with a percentage increase of late apoptotic cells from 0.81% to 13.96%. The cell counts in B1 and B2 quadrants were considered to be apoptotic cells, and the total percentages were 0.98%, 43.99%, 55.75%, and 66.54%, respectively (Fig. 6b). The results demonstrated that the most active derivative **21a** induced cellular apoptosis and thus, as expected, caused the antitumor effects.

2.2.4. Microtubule assembly/depolymerization assay

Combretastatin and its derivatives are recognized as tubulin binding agents with damaging effects on vasculature.^{24,25} In Figure 7, the effect of **21a** on microtubule assembly was analyzed by transmission electron microscope studies. Normal interphase microtubules in dimethylsulfoxide (DMSO) solution exhibited typical reticular formation (Fig. 7A) of polymerization state at 37 °C. In the presence of a high concentration (3 μM) of **21a**, the microtubule polymerization was disturbed (Fig. 7B). The complete depolymerization of microtubules is illustrated in Figure 7B, and a discrete club-shaped tubulin cytoskeleton was observed. The depolymerizing effects of **21a** provide evidence that loss of microtubule function in interphase cells treated with **21a** may prevent these cells from progressing into mitosis. In summary, the correlation between microtubule depolymerization and cancer cell growth inhibition indicates a tight linkage of antiproliferative effects with tubulin-dependent mechanisms of action. The antiproliferative activity of these compounds may derive from their interaction with tubulin and interference with microtubule assembly. Compounds that effectively interfere with tubulin dynamics prevent mitosis in cancer cells, leading to cell cycle arrest and, eventually, apoptosis.

3. Conclusions

In summary, two series (**14a–d** and **21a–h**) of novel spin-labeled derivatives of AVE8063 were synthesized and their in vitro anticancer activity was tested against four tumor cell lines using a MTT assay. The results showed that most of the new spin-labeled compounds exhibited more potent cytotoxicity against four tumor cell lines compared to etoposide, a clinically available anticancer drug, although they were less potent than **3**. Compounds **21a–c** exhibited the highest potency against three tested tumor cell lines (HEPG-2, BGC-832, and HeLa), with IC₅₀ values ranging from 0.15 to 1.05 μM, compared with values of 0.014–0.403 μM for **3**). Compound **21a** was further selected as a representative compound to investigate the antitumor mechanisms of these synthetic compounds. In cell cycle and apoptosis analyses, compound **21a** strongly inhibited the proliferation of HeLa cancer cells, resulting in a massive accumulation of cells in the G2/M phase and inducing a high level of apoptosis. Compound **21a** exhibited strong levels of tubulin depolymerization in the microtubule assembly assay. All of the above results indicated that these synthesized compounds effectively interfered with tubulin dynamics and prevented mitosis in cancer cells, thus, leading to cell cycle arrest and, eventually, dose-dependent apoptosis. These studies suggest that compounds **21a–c** merit further investigation for development as anticancer clinical trial candidates.

4. Experimental section

4.1. General

Melting points were taken on a Kofler melting point apparatus and were uncorrected. Mass spectra were recorded on ZAB-HS and Bruker Daltonics APEXII49e instruments. NMR spectra were recorded on a Bruker AM-400 spectrometer at 400 MHz using TMS as reference (Bruker Company, USA). The electron spin resonance (ESR) spectra were obtained with a Bruker A300 X-band EPR spectrometer. IR spectra were measured on a Nicolet 5DX-FT-IR spectrometer on neat samples placed between KBr plates. The synthetic compounds were purified by flash chromatography on Merck silica gel (70–230 mesh). Thin-layer chromatography (TLC) was performed on silica gel plates with a fluorescent indicator (Merck Silica Gel 60 F₂₅₄ 0.25 mm thick). *N*-(1-Oxyl-2,2,6,6-tet-

ramethyl-4-piperidinyloxycarbonyl)-amino acids were synthesized by employing our previous procedures.²²

4.2. Synthesis of the intermediate 12

A mixture of 3,4,5-trimethoxyphenylacetic acid (8.84 mmol) and 3-nitro-4-methoxybenzaldehyde (4.4 mmol), acetic anhydride (4 mL) and triethylamine (2 mL) were heated under reflux for 3 h. After acidification with concentrated hydrochloric acid (6 mL), the resulting solid was filtered off and recrystallised from ethanol to give acrylic acid intermediate **11** as fine yellow needles. Subsequently the corresponding acrylic acid intermediate (5.56 mmol) was added to powdered copper (28.8 mmol) in quinoline (20 mL), and the resulting mixture was heated at 140 °C for 2 h. Upon cooling, diethyl ether was added, and the copper was filtered off through Celite. The filtrate was washed with 1 M hydrochloric acid, and the aqueous layer was separated and extracted with diethyl ether. The combined organic layers were washed with saturated aqueous sodium carbonate, water, brine, dried (MgSO₄), and concentrated in vacuo. Flash column chromatography (SiO₂ petrol/EtOAc 7:3) and recrystallization from EtOAc and petrol afforded desired intermediate compound **12** in 52% yields, yellow crystals, mp 123–124 °C; ¹H NMR (CDCl₃, 400 MHz) δ: 7.79 (1H, d, *J* = 2.1), 7.42 (1H, dd, *J* = 2.1, 8.7), 6.94 (1H, d, *J* = 8.7), 6.57 (1H, d, *J* = 12.9), 6.47 (2H, s), 6.44 (1H, d, *J* = 12.9), 3.93 (3H, s), 3.85 (3H, s), 3.71 (6H, s); ESI: *m/z*: 346 [M+H]⁺; HRMS calcd 345.1212, found 345.1236.

4.3. Synthesis of the intermediate 3 (AVE8063) from 12

To a solution of compound **12** (2.0 mmol) in HOAc (60 mL) was added zinc powder (32 g). The reaction mixture was stirred at room temperature for 1 h. The reaction mixture was filtered over Celite, and the filtrate was evaporated to dryness. After concentration, the residue was purified by silica gel column chromatography (CH₂Cl₂) to give pure product in 45% yields. ¹H NMR (CDCl₃, 400 MHz) δ: 6.69 (1H, s), 6.67 (2H, s), 6.55 (2H, s), 6.45 (1H, d, *J* = 12.0), 6.36 (1H, d, *J* = 12.0), 3.84 (3H, s), 3.82 (3H, s), 3.69 (6H, s); ESI: *m/z*: 316 [M+1]; HRMS calcd 315.1471, found 315.1457.

4.4. General procedure for synthesis of target compounds 14a–d

A mixture of the appropriate piperidine (pyrrolidine) nitroxyl acids (0.5 mmol), compound **3** (0.5 mmol) and DMAP (20 mg) was stirred in anhydrous CH₂Cl₂ (20 mL) for 5 min at room temperature under nitrogen. DCC (106 mg, 0.5 mmol) was added and the mixture was stirred for 24 h. The reaction mixture was filtered and the filtrate was evaporated. The residue was subjected to column chromatography on silica gel with CH₂Cl₂–acetone to afford target compounds **14a–d**, and their structures were confirmed from mp, IR, ESR and HRMS analyses.

4.4.1. 3'-N-(1''-Oxyl-2'',2'',5'',5''-tetramethyl-3''-pyrrolidinyloxycarbonyl)-amido-AVE8063 (14a)

Yellow powder, yield: 33%; mp 126–127 °C. IR (KBr) cm⁻¹: 3424, 2972, 2928, 2852, 1675, 1530, 1504, 1459, 1360 (N–O), 1126; ESR: An = 14.70 G, *g*₀ = 2.0055; MS (ESI) *m/z*: 482 [M+H]⁺, HRMS: *m/z* calcd for C₂₇H₃₃N₂O₆: 482.2411 [M+H]⁺, found 482.2418 [M+H]⁺.

4.4.2. 3'-N-(1''-Oxyl-2'',2'',5'',5''-tetramethyl-3''-pyrrolidinyloxycarbonyl)-amido-AVE8063 (14b)

Yellow powder, yield: 39%; mp 128–129 °C. IR (KBr) cm⁻¹: 3420, 2972, 2930, 2846, 1687, 1532, 1504, 1460, 1365 (N–O), 1127; ESR: An = 15.28 G, *g*₀ = 2.0061; MS (ESI) *m/z*: 484 [M+H]⁺;

HRMS: *m/z* calcd for C₂₇H₃₅N₂O₆: 484.2568 [M+H]⁺, found 484.2556 [M+H]⁺.

4.4.3. 3'-N-(1''-Oxyl-2'',2'',6'',6''-tetramethyl-4''-tetrahydropyridinyloxycarbonyl)-amido-AVE8063 (14c)

Red powder, yield: 64%; mp 93–95 °C. IR (KBr) cm⁻¹: 3426, 2970, 2931, 2849, 1679, 1531, 1505, 1459, 1360 (N–O), 1127; ESR: An = 14.62 G, *g*₀ = 2.0055; MS (ESI) *m/z*: 496 [M+H]⁺; HRMS: *m/z* calcd for C₂₈H₃₅N₂O₆: 496.2568 [M+H]⁺, found 496.2559 [M+H]⁺.

4.4.4. 3'-N-(1''-Oxyl-2'',2'',6'',6''-tetramethyl-4''-piperidinyloxycarbonyl)-amido-AVE8063 (14d)

Red powder, yield: 76%; mp 146–148 °C. IR (KBr) cm⁻¹: 3334, 2929, 2852, 1683, 1535, 1505, 1458, 1362 (N–O), 1126; ESR: An = 15.76 G, *g*₀ = 2.0058; MS (ESI) *m/z*: 498 [M+H]⁺; HRMS: *m/z* calcd for C₂₈H₃₇N₂O₆: 498.2724 [M+H]⁺, found 498.2711 [M+H]⁺.

4.5. General procedure for synthesis of target compounds 21a–h

The corresponding *N*-(1-oxyl-2,2,6,6-tetramethyl-4-piperidinyloxycarbonyl) amino acids **20a–h** (0.47 mmol) were dissolved in 50 mL of anhydrous CH₂Cl₂ and cooled to 0 °C. 1-Hydroxybenzotriazole (HOBt) (0.7 mmol) and EDCI (0.56 mmol) were added, and the mixture was stirred for 30 min at 0 °C. Subsequently, 0.39 mmol of compound **3** and finally 2.4 mL of *N*-ethyl diisopropylamine were added. The mixture was stirred for 16 h at ambient temperature. The solvent was removed under reduced pressure and the residue was purified by flask-column chromatography (gradient elution with mixtures of chloroform/methanol) on silica gel as monitored by TLC. Synthesized target compounds **21a–h** were characterized by mp, IR, ESR and HRMS analyses.

4.5.1. 3'-N-[N-(1''-Oxyl-2'',2'',6'',6''-tetramethyl-4''-piperidinyloxycarbonyl)-L-glycyl]-amido-AVE8063 (21a)

Red powder, yield: 72%; mp 77–79 °C; IR (KBr) cm⁻¹: 3397, 3331, 2972, 2934, 2853, 1723, 1696, 1637, 1584, 1535, 1507, 1460, 1363(N–O), 1326, 1239, 1126, 1012; ESR: An = 16.02 G, *g*₀ = 2.0061; MS *m/z*: 571 [M+H]⁺; HRMS: *m/z* calcd for C₃₀H₄₀N₃O₈: 593.2708 [M+Na]⁺, found 593.2716 [M+Na]⁺.

4.5.2. 3'-N-[N-(1''-Oxyl-2'',2'',6'',6''-tetramethyl-4''-piperidinyloxycarbonyl)-L-alanyl]-amido-AVE8063 (21b)

Red powder, yield: 68%; mp 75–77 °C; IR (KBr) 3400, 3327, 2974, 2936, 2838, 1722, 1699, 1628, 1584, 1533, 1506, 1459, 1360 (N–O), 1326, 1239, 1126, 1028; ESR: An = 16.16 G, *g*₀ = 2.006; MS *m/z*: 585 [M+H]⁺; HRMS: *m/z* calcd for C₃₁H₄₂N₃O₈: 607.2864 [M+Na]⁺, found 607.2855 [M+Na]⁺.

4.5.3. 3'-N-[N-(1''-Oxyl-2'',2'',6'',6''-tetramethyl-4''-piperidinyloxycarbonyl)-L-valinyl]-amido-AVE8063 (21c)

Red powder, yield: 75%; mp 75–77 °C; IR (KBr) cm⁻¹: 3327, 2968, 2931, 2851, 1717, 1685, 1629, 1581, 1533, 1505, 1463, 1363(N–O), 1325, 1238, 1127, 1025; ESR: An = 16.04 G, *g*₀ = 2.0061; MS *m/z*: 613 [M+H]⁺; HRMS: *m/z* calcd for C₃₃H₄₆N₃O₈: 635.3177 [M+Na]⁺, found 635.3188 [M+Na]⁺.

4.5.4. 3'-N-[N-(1''-Oxyl-2'',2'',6'',6''-tetramethyl-4''-piperidinyloxycarbonyl)-L-methioninyl]-amido-AVE8063 (21d)

Red powder, yield: 60%; mp 72–73 °C; IR (KBr) cm⁻¹: 3397, 3324, 2971, 2934, 2840, 1718, 1688, 1583, 1534, 1507, 1459, 1363 (N–O), 1326, 1238, 1126, 1030; ESR: An = 15.78 G, *g*₀ = 2.0061; MS *m/z*: 645 [M+H]⁺; HRMS: *m/z* calcd for C₃₃H₄₆N₃S₂O₈: 667.2898 [M+Na]⁺, found 667.2880 [M+Na]⁺.

4.5.5. 3'-N-[N-(1''-Oxyl-2'',2'',6'',6''-tetramethyl-4''-piperidinylcarbonyl)-L-isoleuciny]-amido-AVE8063 (21e)

Red powder, yield: 70%; mp 62–64 °C; IR (KBr) cm^{-1} : 3397, 3324, 2968, 2934, 2878, 1709, 1684, 1627, 1583, 1535, 1506, 1461, 1362 (N–O), 1236, 1127, 1026; ESR: An = 16.10 G, $g_0 = 2.006$; MS m/z : 627 [M+H]⁺; HRMS: m/z calcd for C₃₃H₄₈N₃O₈: 649.3334 [M+Na]⁺, found 649.3318 [M+Na]⁺.

4.5.6. 3'-N-[N-(1''-Oxyl-2'',2'',6'',6''-tetramethyl-4''-piperidinylcarbonyl)-L-prolinyl]-amido-AVE8063 (21f)

Red powder, yield: 64%; mp 51–52 °C; IR (KBr) cm^{-1} : 3402, 3327, 2973, 2936, 2838, 1697, 1583, 1534, 1503, 1461, 1417, 1366 (N–O), 1327, 1241, 1124, 1027; ESR: An = 15.88 G, $g_0 = 2.006$; MS m/z : 611 [M+H]⁺; HRMS: m/z calcd for C₃₃H₄₄N₃O₈: 633.3021 [M+Na]⁺, found 633.3037 [M+Na]⁺.

4.5.7. 3'-N-[N-(1''-Oxyl-2'',2'',6'',6''-tetramethyl-4''-piperidinylcarbonyl)-L-phenylalaninyl]-amido-AVE8063 (21g)

Red powder, yield: 70%; mp 78–80 °C; IR (KBr) cm^{-1} : 3400, 3324, 2972, 2935, 2838, 1717, 1690, 1627, 1583, 1535, 1504, 1458, 1361(N–O), 1326, 1239, 1125, 1029; ESR: An = 15.98 G, $g_0 = 2.006$; MS m/z : 661[M+H]⁺; HRMS: m/z calcd for C₃₇H₄₆N₃O₈: 683.3177 [M+Na]⁺, found 683.3166 [M+Na]⁺.

4.5.8. 3'-N-[N-(1''-Oxyl-2'',2'',6'',6''-tetramethyl-4''-piperidinylcarbonyl)-L-tyrosinyl]-amido-AVE8063 (21h)

Red powder, yield: 55%; mp 96–97 °C; IR (KBr) cm^{-1} : 3404, 3329, 2970, 2931, 2849, 1713, 1690, 1626, 1582, 1533, 1504, 1458, 1364 (N–O), 1327, 1238, 1125, 1028; ESR: An = 15.78 G, $g_0 = 2.0061$; MS m/z : 700 [M+H]⁺; HRMS: m/z calcd for C₃₉H₄₇N₄O₈: 722.3286 [M+Na]⁺, found 722.3279 [M+Na]⁺.

4.6. Biological assay**4.6.1. Cell culture and inhibition of cell growth**

Four independent human tumor cell lines, K562 leukemia, SGC-7901 gastric cancer, HeLa cervical carcinoma and HepG2 hepatocellular liver carcinoma, were obtained from Key Lab of Preclinical Study for New Drugs, Lanzhou University, Gansu Province. All test compounds were dissolved in DMSO at 1 mg/mL immediately before use and diluted in the medium before addition to the cells. All cell lines were cultured in an RPMI 1640 medium (GIBCO) supplemented with 10% bovine fetal calf serum, 2 mM L-glutamine (GIBCO), 10 mM β-mercaptoethanol, 100 U/mL of penicillin and 100 μg/mL of streptomycin. Cells (2 × 10⁵ cells in 100 mL medium) in their log phase of growth were seeded in 96-well microtitre plates. After 24 h of incubation at 37 °C and 5% CO₂ to allow cell attachment, cultures were treated with varying concentrations (0–100 μM) of test compounds. For each concentration, five replicate wells were used. Considering the possible antiproliferative effects of DMSO, the concentration of DMSO in the array was less than 0.1% and would not affect the cell growth of the cell lines. The cell growth was calculated by subtracting the mean OD value of the respective blank from the mean OD value of the experimental set. Percentage of growth in the presence of test compounds was calculated considering the growth in the absence of any test compounds as 100%, and the results are reported in terms of IC₅₀ (concentration causing 50% inhibition relative to untreated controls) values.

4.6.2. Cell cycle analysis and apoptosis detection

Flow cytometry was used to measure cell cycle profile and apoptosis. For cell cycle analysis, HeLa cells (1 × 10⁵) treated with compounds **21a** with various concentrations (0, 0.375, 1.5, and 3 μM) were washed twice with ice-cold PBS, harvested, fixed with ice cold PBS in 70% ethanol and stored at –20 °C for 30 min. After

fixation, these cells were incubated with RNase A (0.1 mg/mL) at 37 °C for 30 min, and then stained with propidium iodide (50 μg/mL) for 30 min on ice in the dark. Cells were harvested by centrifugation and further stained with DNA staining solution (10 mg). The DNA contents were then detected by flow cytometer and the cell cycle profile was analyzed from the DNA content histograms.²⁶

4.6.3. Flow cytometry with FITC-Annexin V/PI double staining

Trypsin (Sigma) without EDTA was used to digest and collect the control group and the cells treated with 0.375, 1.5, and 3 μM of compound **21a**. Flow cytometry was performed according to the apoptosis detection kit procedures. The HeLa cells were washed twice with PBS and centrifuged at 300×g for 5 min. 5 × 10⁵ cells were collected. Binding buffer suspension (500 μL) was added to the cells, and then 5 μL of the FITC-Annexin V mix was added. Next, 5 μL of the PI mix was added, and the suspension was mixed and kept at room temperature in the dark for 15 min of reaction. Flow cytometry was performed using a FACSC alibur Xow cytometer (BD Biosciences, CA, USA).

4.6.4. Separation of active microtubule protein

Goat brain (1.8 kg) was homogenized in a Waring blender and then centrifuged in the cold at 32,800 rpm for 1 h. The supernatant was decanted and divided into four aliquots. ATP and GTP were added to the aliquots at 37 °C, incubated, and centrifuged. The supernatants were discarded, and the pellets were homogenized. After 30 min on ice, the viscous suspension was centrifuged in the cold for 30 min. The pellet was re-homogenized sequentially two times and the cold centrifugation was repeated each time. All supernatants were pooled and the cold pellets were set aside. To each 100 mL of the combined supernatant were added 55.3 g of glycerol (4 M) and 5 mL of a solution containing Mes (pH 6.4), EGTA, MgCl₂, 2-mercaptoethanol, and EDTA to maintain the concentrations of these components and ATP and GTP for final concentrations of 1 and 0.3 mM. The mixture was incubated at 37 °C for 1 h and centrifuged with warming for 1 h at 32,000 rpm, and the warm supernatant was set aside. The suspension was left on ice for 30 min and centrifuged in the cold for 30 min. Very small cold pellets were obtained and were combined with the prior cold pellets.²⁷

4.6.5. In vitro tubulin polymerization analysis

Electron micrographs were used to observe the depolymerization state of the tubulin protein. Tubulins were incubated with or without compound **21a** in assay buffer (80 mM PIPES (pH 6.9), 1 mM MgCl₂, and 1 mM EDTA) containing 30% glycerol and 1 mM GTP for 30 min at 37 °C. Samples were fixed by dilution (1:20- to 1:50-fold) into assay buffer containing 30% glycerol and 0.5% glutaraldehyde at 37 °C, and then 10 mL of each sample were spotted onto Formavar-coated grids and stained with uranyl acetate for 30 s. Electron micrographs were obtained using a Philips CM-12 transmission electron microscope with an accelerating voltage of 100 kV.

Acknowledgments

This work was financially supported by the National Natural Science Foundation of China (30800720); Project supported by the Young Scholars Science Foundation of Lanzhou Jiaotong University (2011011); the Post-Doctor Research Foundation (20090450142); the Fundamental Research Funds for the Central Universities (Izujbky-2009-98).

References and notes

1. Cirila, A.; Mann, J. *Nat. Prod. Rep.* **2003**, *20*, 558.

2. Nam, N. H. *Curr. Med. Chem.* **2003**, *10*, 1697.
3. Tron, G. C.; Pirali, T.; Sorba, G.; Pagliai, F.; Busacca, S.; Genazzani, A. A. *J. Med. Chem.* **2006**, *49*, 3033.
4. Siemann, D. W.; Chaplin, D. J.; Walicke, P. A. *Expert Opin. Invest. Drugs* **2009**, *18*, 189.
5. Tozer, G. M.; Kanthou, C.; Parkins, C. S.; Hill, S. A. *Int. J. Exp. Pathol.* **2002**, *83*, 21.
6. Chaudhary, A.; Pandeya, S. N.; Kumar, P.; Sharma, P. P.; Gupta, S.; Soni, N.; Verma, K. K.; Bhardwaj, G. *Mini-Rev. Med. Chem.* **2007**, *7*, 1186.
7. Naik, N.; Braslau, R. Synthesis and applications of optically active nitroxides *Tetrahedron* **1998**, *54*, 99.
8. Soule, -B. P.; Hyodo, F.; Matsumoto, K.; Simone, N. L.; Cook, J. A.; Krishna, M. C.; Mitchell, J. B. *Free Radical Biol. Med.* **2007**, *42*, 1632.
9. Raikov, Z. D.; Atanasov, A. T.; Raikova, E. T. *Med. Hypotheses* **2003**, *60*, 387.
10. Gadjeva, V. G. *Int. J. Pharm.* **2002**, *247*, 39.
11. Zheleva, A.; Stanilova, S.; Dobreva, Z.; Zhelev, Z. *Int. J. Pharm.* **2001**, *222*, 237.
12. Liu, Y. Q.; Tian, X.; Yang, L.; Zhan, Z. C. *Europ. J. Med. Chem.* **2008**, *43*, 2610.
13. Tian, X.; Wang, Y. G.; Yang, M. G.; Chen, Y. Z. *Life Sci.* **1997**, *60*, 511.
14. Jin, Y.; Chen, S. W.; Tian, X. *Bioorg. Med. Chem.* **2006**, *14*, 3062.
15. Tian, X.; Zhang, F. M.; Li, W. G. *Life Sci.* **2002**, *70*, 2433.
16. Zhang, Z. W.; Zhang, J. Q.; Hui, L.; Chen, S. W.; Tian, X. *Europ. J. Med. Chem.* **2010**, *45*, 1673.
17. Liu, Y. Q.; Ohkoshi, E.; Li, L. H.; Yang, L.; Lee, K. H. *Bioorg. Med. Chem. Lett.* **2012**, *22*, 920.
18. Liu, Y. Q.; Yang, L.; Tian, X. *Curr. Bioact. Compd.* **2007**, *3*, 73.
19. Li, X. J.; Yang, L.; Liu, Y. Q.; Li, C. *Nat. Prod. Res.* **2012**, *26*, 1271.
20. Gaukroger, K.; Hadfield, J. A.; Hepworth, L. A.; Lawrence, N. J.; McGown, A. T. *J. Org. Chem.* **2001**, *66*, 8135.
21. Pettit, G. R.; Anderson, C. R.; Herald, D. L.; Jung, M. K.; Lee, D. J.; Hamel, E.; Pettit, R. K. *J. Med. Chem.* **2003**, *46*, 525.
22. Liu, Y. Q.; Tian, X. *Synth. Commun.* **2005**, *35*, 2749.
23. Rubinstein, L. V.; Shoemaker, R. H.; Paull, K. D. *J. Natl. Cancer Inst.* **1990**, *82*, 1113.
24. Pettit, G. R.; Singh, S. B.; Hamel, E.; Lin, C. M.; Alberts, D. S.; Garcia-Kendall, D. *Experientia* **1989**, *45*, 209.
25. Lin, C. M.; Ho, H. H.; Pettit, G. R.; Hamel, E. *Biochemistry* **1989**, *28*, 6984.
26. Gambari, R.; Terada, M.; Bank, A.; Rifkind, R. A.; Marks, P. A. *Proc. Natl. Acad. Sci. U.S.A.* **1978**, *75*, 3801.
27. Hamel, E.; Lin, C. M. *Biochemistry* **1984**, *23*, 4173.